Physics Letters B 666 (2008) 425–429

Contents lists available at ScienceDirect

Physics Letters B

www.elsevier.com/locate/physletb

# Modification of the $\rho$ meson detected by low-mass electron–positron pairs in central Pb–Au collisions at 158*A* GeV/*c*

CERES Collaboration

D. Adamová [a], G. Agakichiev [b], D. Antończyk [b], H. Appelshäuser [c,*], V. Belaga [d], J. Bielcikova [e], P. Braun-Munzinger [b], O. Busch [b], A. Cherlin [f], S. Damjanović [e], T. Dietel [e], L. Dietrich [e], A. Drees [g], W. Dubitzky [e], S.I. Esumi [e], K. Filimonov [e], K. Fomenko [d], Z. Fraenkel [f,✠], C. Garabatos [b], P. Glässel [e], J. Holeczek [b], V. Kushpil [a], A. Maas [b], A. Marín [b], J. Milošević [e], A. Milov [f], D. Miśkowiec [b], Yu. Panebrattsev [d], O. Petchenova [d], V. Petráček [e], A. Pfeiffer [h], J. Rak [i], I. Ravinovich [f], P. Rehak [j], H. Sako [b], W. Schmitz [e], S. Sedykh [b], S. Shimansky [d], J. Stachel [e], M. Šumbera [a], H. Tilsner [e], I. Tserruya [f], J.P. Wessels [k], T. Wienold [e], J.P. Wurm [i], W. Xie [f], S. Yurevich [e], V. Yurevich [d]

[a] *Nuclear Physics Institute ASCR, 25068 Řež, Czech Republic*
[b] *Gesellschaft für Schwerionenforschung (GSI), D-64291 Darmstadt, Germany*
[c] *Institut für Kernphysik der Universität Frankfurt, D-60486 Frankfurt, Germany*
[d] *Joint Institute for Nuclear Research, 141980 Dubna, Russia*
[e] *Physikalisches Institut der Universität Heidelberg, D-69120 Heidelberg, Germany*
[f] *Weizmann Institute, Rehovot 76100, Israel*
[g] *Department of Physics and Astronomy, State University of New York–Stony Brook, Stony Brook, NY 11794-3800, USA*
[h] *CERN, 1211 Geneva 23, Switzerland*
[i] *Max-Planck-Institut für Kernphysik, D-69117 Heidelberg, Germany*
[j] *Brookhaven National Laboratory, Upton, NY 11973-5000, USA*
[k] *Institut für Kernphysik der Universität Münster, D-48149 Münster, Germany*

ARTICLE INFO

*Article history:*
Received 15 November 2006
Received in revised form 28 July 2008
Accepted 29 July 2008
Available online 7 August 2008
Editor: V. Metag

*PACS:*
25.75.-q
25.75.Gz

ABSTRACT

We present a measurement of $e^+e^-$ pair production in central Pb–Au collisions at 158*A* GeV/*c*. As reported earlier, a significant excess of the $e^+e^-$ pair yield over the expectation from hadron decays is observed. The improved mass resolution of the present data set, recorded with the upgraded CERES experiment at the CERN-SPS, allows for a comparison of the data with different theoretical approaches. The data clearly favor a substantial in-medium broadening of the $\rho$ spectral function over a density-dependent shift of the $\rho$ pole mass. The in-medium broadening model implies that baryon induced interactions are the key mechanism to the observed modifications of the $\rho$ meson at SPS energy.



## 1. Introduction

The masses of hadrons are created dynamically by the strong interaction, when confinement forces quarks and gluons to form color-neutral bound states. The generation of hadronic masses is connected to spontaneous chiral symmetry breaking, a basic feature of the vacuum structure of Quantum-Chromo-Dynamics (QCD). Evidently, the mechanism of chiral symmetry breaking is of fundamental importance for the properties of matter in the universe. However, the quantitative understanding of the dynamics in this non-perturbative regime of QCD is still rather incomplete, and additional information from experiment is essential.

According to investigations of the non-perturbative properties of QCD on a discrete space–time lattice a plasma of deconfined quarks and gluons (QGP) should be formed at energy densities $\epsilon \geqslant 1$ GeV/fm$^3$. Simultaneously with this deconfinement transition, chiral symmetry is expected to be restored (see [1] for a recent review). In collisions of heavy nuclei at high energies such energy densities are exceeded significantly and there is by now strong, albeit indirect evidence for the formation of a QGP (for recent reviews see [2–5]). On the way to chiral symmetry restoration in such matter, significant modifications of the properties of hadrons are expected [6,7], such as of their mass and width or more generally of the hadronic spectral function.

* Corresponding author.
*E-mail address:* appels@ikf.uni-frankfurt.de (H. Appelshäuser).
✠ Deceased.

0370-2693 
doi:10.1016/j.physletb.2008.07.104

The $\rho$ meson ($J^P = 1^-$) is an ideal probe to investigate modifications of such in-medium properties. In a hot hadronic medium close to the phase boundary, $\rho$ mesons are abundantly produced by annihilation of thermal pions. Due to its short lifetime ($c\tau = 1.3$ fm), the decay of the $\rho$ meson occurs inside the medium, and spectral modifications may be observable via the kinematic reconstruction of the decay products. Finally, its decay into lepton pairs provides essentially undisturbed information from the hot and dense phase, because leptons are not subject to final state rescattering in the strongly interacting medium.

Enhanced low-mass $e^+e^-$ pair production in nucleus–nucleus collisions at full energy of the CERN-Super-Proton-Synchrotron (SPS) has been reported by the CERES experiment. In particular, in the mass region 0.2–0.6 GeV/$c^2$, the measured di-lepton yield exceeds expectations from hadron decays by a factor 2–3 [8–10]. Even bigger enhancement factors have been found at 40$A$ GeV/$c$ [11], albeit with large statistical uncertainties. At RHIC energies, enhancement factors similar to those observed at the top SPS energy have been reported recently [12].

Significant $\rho$ meson production via annihilation of thermal pions in the hot and dense hadronic medium is a likely mechanism for enhanced electron pair production. Implementing this mechanism, substantial temperature and baryon density dependent modifications of the $\rho$-spectral function [7,13,14] needed to be considered to explain the mass spectrum of the pair enhancement. However, the detailed behaviour of the spectral function as chiral symmetry is restored is still up to speculation. Quite different theoretical approaches exist which could not be discriminated by the previous di-electron data.

The NA60 Collaboration recently corroborated previous CERES findings and reported a significant di-muon excess in nucleus–nucleus collisions over the expectation from hadronic decays [15]. The NA60 measurement of the di-muon excess in $^{115}$In–In collisions at 158$A$ GeV/$c$ favors models including significant broadening but no mass shift of the $\rho$-spectral function [15,16].

## 2. Experiment and data analysis

In this Letter, we present results on $e^+e^-$ pair production in central $^{208}$Pb–$^{197}$Au collisions at 158$A$ GeV/$c$. The data have been recorded by the CERES experiment at the SPS in the year 2000 [17]. Typically, $10^6$ lead ions per 5.2 s extraction cycle were focused on 13 thin gold targets aligned along the beam line (25 μm each, totalling 1.2% of a nuclear interaction length). The interaction vertex was reconstructed using charged particle track segments from two silicon drift detectors (SDD) placed 10.4 and 14.3 cm downstream of the target. Electrons are identified by their ring signature in two RICH detectors, which are blind to hadrons below $p \approx 4.5$ GeV/$c$ ($\gamma_{\text{thresh}} \approx 32$). The experimental setup was upgraded by a downstream radial drift Time Projection Chamber (TPC) which is operated inside an inhomogeneous magnetic field with a radial component of up to 0.75 T. Employing tracking information from the TPC, the mass resolution of the spectrometer was improved to $\Delta m/m = 3.8\%$ in the region of the $\phi$ meson mass [17]. The resolution has been determined by a Monte Carlo procedure where simulated tracks were embedded into real data events. This method provides a detailed simulation of the TPC response to charged particles in a realistic track density environment. The same Monte Carlo describes very well the experimentally observed peak width of the $K_s^0$ reconstructed in the $\pi^+\pi^-$ channel ($\sigma_{K_s^0 \to \pi^+\pi^-} \approx 15$ MeV/$c^2$). The TPC also provides additional electron identification via measurement of the specific energy loss d$E$/d$x$ with a resolution of about 10%. The spectrometer provides full azimuthal acceptance in the pseudorapidity range $2.1 < \eta < 2.65$.

The present results are based on an analysis [18–20] of 25 million Pb–Au events, selected at a centrality of $\sigma/\sigma_{\text{geo}} = 7\%$ [21]. SDD track segments are matched to charged particle tracks in the TPC, where the deflection in the magnetic field determines the momentum with a resolution of $\Delta p/p \approx ((2\%)^2 + (1\% \cdot p(\text{GeV}/c))^2)^{1/2}$ [17]. Combined electron information from cuts on the ring quality in the RICH detectors and TPC d$E$/d$x$ leads to a pion suppression of typically $4 \times 10^4$ at 67% electron efficiency [18].

A set of cuts is applied to the track candidates to minimize the amount of combinatorial background from unrecognized Dalitz pairs and conversions, making use of their characteristic decay topology. Electron and positron tracks are rejected if their d$E$/d$x$ significantly exceeds that of a single track in both SDDs, indicating an unresolved close pair. Also, electron and positron tracks are rejected if a soft track with opposite charge and electron-like d$E$/d$x$ is found in the TPC at small angular separation.

The remaining electron and positron tracks are then combined into pairs. To further suppress combinatorial background, tracks which form pairs with opening angle smaller than 35 mrad are treated as recognized conversions or Dalitz pairs and are not used for further pairing. Finally, a low transverse momentum cut of 0.2 GeV/$c$ is applied to all electron and positron tracks.

The single-electron reconstruction efficiency has been determined by a Monte Carlo (MC) procedure where simulated tracks are embedded into real raw data events. The subsequent analysis of the MC sample includes all cuts and methods as applied to the real data. The final pair reconstruction efficiency $\epsilon_{\text{ee}}$ is typically 14%. It depends on the polar angles of the single tracks and (slightly) on centrality. The efficiency correction is performed by assigning a weight $w_{\text{ee}}$ to each pair which is the inverse of the pair reconstruction efficiency $\epsilon_{\text{ee}}$. The pair reconstruction efficiency is calculated from the single track efficiencies, using the parametrized dependencies on track polar angle $\theta$ and charged particle multiplicity $N_{\text{ch}}$:

$$w_{\text{ee}} = \frac{1}{\epsilon_{\text{ee}}} = \frac{1}{\epsilon_{\text{track1}}(\theta_1, N_{\text{ch}}) \cdot \epsilon_{\text{track2}}(\theta_2, N_{\text{ch}})}. \tag{1}$$

Based on a systematic variation of the cut values in the MC, the systematic uncertainty on the pair reconstruction efficiency is estimated to 8.4%.

The remaining combinatorial background is estimated to equal the number of like-sign lepton pairs from the same event. The limited statistics of the like-sign pair sample adds a significant statistical error to the final result. Alternatively, a mixed-event technique can be applied, where unlike-sign pairs are formed from electron and positron tracks of different events and the corresponding mixed-event spectrum is normalized to the same-event like-sign yield. This approach reduces considerably the statistical bin-to-bin fluctuations but bears a statistical and systematic uncertainty due to the normalization procedure. The normalization constant is determined by the ratio of the mixed-event spectrum to the same-event like-sign spectrum. The statistical accuracy of the normalization is limited by the number of counts in the same-event like-sign spectrum and yields about $4 \times 10^{-3}$. The uncertainty in the normalization of the background has been included in the systematic error of the final dilepton yield. The magnitude of this contribution after background subtraction depends on the signal-to-background ratio and yields typically 8.8% at $S/B = 1/22$ (see below).

We found that the final results using the like-sign and the mixed-event sample are in good agreement within statistical errors [18]. Small deviations are only visible at invariant masses below 0.1 GeV/$c^2$. This is caused by limitations of the two-ring separation, which are only present in the same-event sample. To account for this effect, which is also present in the 'true' unlike-sign combinatorial background, we have used the same-event like-sign background estimate for masses below 0.2 GeV/$c^2$. No statistical limitation is imposed by this procedure, since the signal-

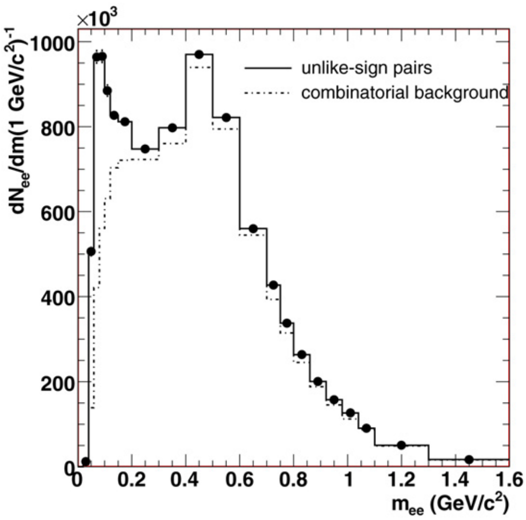


**Fig. 1.** Unlike-sign pair yield (histogram) and combinatorial background (dashed curve). See text for explanation.

to-background ratio is very good in this mass region. For masses greater than 0.2 GeV/$c^2$, the normalized mixed-event unlike-sign sample is used for background subtraction. The resulting background distribution and the unlike-sign signal pair spectrum after efficiency correction are shown in Fig. 1.

Below $m_{ee} = 0.2$ GeV/$c^2$ the $\pi^0$-Dalitz contribution is clearly visible. The raw net yield in this mass range after subtraction of the combinatorial background contains $6114 \pm 176$ electron-positron pairs at a signal-to-background ratio $S/B = 1/2$. At masses larger than 0.2 GeV/$c^2$, the number of pairs contributing to the signal is $3115 \pm 376$ at $S/B = 1/22$.

After background subtraction, the $e^+e^-$ pair yield is normalized to the total number of events and to the average charged particle multiplicity $\langle N_{ch} \rangle$ in the spectrometer acceptance. The average charged particle multiplicity has been determined by the number of tracks in the SDD. For the 7% most central events we obtain $\langle N_{ch} \rangle = 177 \pm 14$ (syst.) in $2.1 < \eta < 2.65$. The systematic error on $\langle N_{ch} \rangle$ adds a contribution of 8% to the total systematic error on the pair yield per charged particle.

The total systematic error of the data is given by (i) the uncertainty of the efficiency determination (8.4%), (ii) the normalization of the mixed-event background ($0.004 \cdot B/S$, on average 8.8%) and (iii) the determination of the charged particle multiplicity (8%). These contributions add up to an average of 14.6%, however, note that contribution (ii) differs bin-by-bin, depending on the local signal-to-background ratio, and applies only for $m_{ee} > 0.2$ GeV/$c^2$.

## 3. Results and discussion

The $e^+e^-$ invariant mass distribution after efficiency correction, combinatorial background subtraction and normalization is shown in Fig. 2(a). Also shown is the 'hadronic cocktail' which comprises the yield from hadronic decays in A–A collisions after chemical freeze-out (see [10]).[1] In the mass range $0.2 < m_{ee} < 1.1$ GeV/$c^2$, the data are enhanced over the cocktail by a factor $2.45 \pm 0.21(\text{stat}) \pm 0.35(\text{syst}) \pm 0.58(\text{decays})$. The last error arises from the systematic uncertainty in the cocktail calculation. The enhancement is most pronounced in the mass region $0.2 < m_{ee} < 0.6$ GeV/$c^2$, in agreement with earlier findings. In contrast to previous CERES results, the improved mass resolution of the upgraded spectrometer provides access to the resonance structure in the $\rho/\omega$ and $\phi$ region. A quantitative study of $\phi$ meson production in the $e^+e^-$ and $K^+K^-$ channels can be found in [22].

In Fig. 2(b) the data are compared with a model approach implying enhanced di-lepton production via thermal pion annihilation and a realistic space–time evolution [24]. The calculated di-lepton yield was filtered by the CERES acceptance and folded with the experimental resolution. Temperature and baryon-density dependent modifications of the $\rho$-spectral function have been taken into account: the dropping mass scenario which assumes a shift of the in-medium $\rho$ mass [7,14], and the broadening scenario where the $\rho$-spectral function is smeared due to coupling to the hadronic medium [13,16]. The calculations include as well contributions from QGP, the Drell–Yan process, and 4-pion annihilation with chiral mixing. The calculations for both spectral functions describe the enhancement reasonably well for masses below 0.7 GeV/$c^2$. In the resonance region, however, there is a notable difference between the calculations. In particular in the mass region between the $\omega$ and the $\phi$, the data clearly favor the broadening scenario over the dropping mass scenario.

In order to exhibit the shape of the in-medium contribution, we subtract the hadronic cocktail (excluding the $\rho$ meson) from the data (Fig. 3). The vacuum $\rho$-decay contribution to the data ("cocktail $\rho$", solid line in Fig. 3) is completely negligible compared to the measurements. The excess data exhibit a very broad structure reaching very low masses and exceed the vacuum $\rho$ contribution by a factor $10.6 \pm 1.3$. The data are compared to model calculations of the in-medium di-electron production. These are normalized, like the measured yield, to the number of charged particles. Note that the model calculations give absolute pair yields (in terms of charged particle numbers) and there is no freedom of adjustment. Yield and spectral shape are well described by the broadening scenario but are not consistent[2] with a dropping $\rho$ mass (Fig. 3(a)). While the dropping mass calculation yields a rather narrow distribution with a peak around 0.5 GeV/$c^2$ the measured excess is spread over a significantly wider mass range. Below 0.2 GeV/$c^2$, the large errors arising from the subtraction of large numbers in the $\pi^0$ Dalitz region do not allow for a definite conclusion. However, the trend indicates a further increase of the in-medium contribution towards the photon point.

A $\chi^2$-analysis of the data in the mass region $0.12 < m_{ee} < 1.1$ GeV/$c^2$ (dof $= 13$) with respect to the model calculations in Fig. 3 results in $\chi^2_{\text{IMH}} = 10.6$ ($P_{\text{IMH(stat)}} = 64.4\%$) for the in-medium hadronic spectral function approach and $\chi^2_{\text{DRM}} = 33.1$ ($P_{\text{DRM(stat)}} = 0.0017\%$) for the dropping $\rho$ mass scenario, if only statistical errors are considered. To judge how well the data resemble the calculations shown in Fig. 3(a) including systematic uncertainties in data and cocktail, a Monte Carlo procedure has been employed. In this procedure, the model curves have been used as input to generate simulated spectra, assuming statistical and systematic uncertainties as in the real data. The total systematic error in each mass bin has been calculated by adding in quadrature the systematic error contributions to data and cocktail. The resulting total systematic error is interpreted as a Gaussian standard deviation of a coherent up- or downward shift of all data points in the spectrum. Statistical point-to-point fluctuations have been added according to the statistical error bars of the real data. For each of the generated spectra, the $\chi^2$-value with respect to the input model curve has been calculated. Finally, the probability to obtain a $\chi^2$-value which is larger than the one observed in the data has been determined for each of the two model curves. We obtain $P_{\text{IMH}} = 81.1\%$ for the

[1] For the $\phi$ meson we use 70% of the thermal model yield, in accordance with measurements [22]. The calculation of the present cocktail includes also the recently improved branching ratio for $\omega \to \pi^0 e^+e^-$ [23].

[2] Recently, Brown et al. [26] have advocated a different view in which their scaling is not directly related anymore to the shape of the low mass di-lepton spectrum.

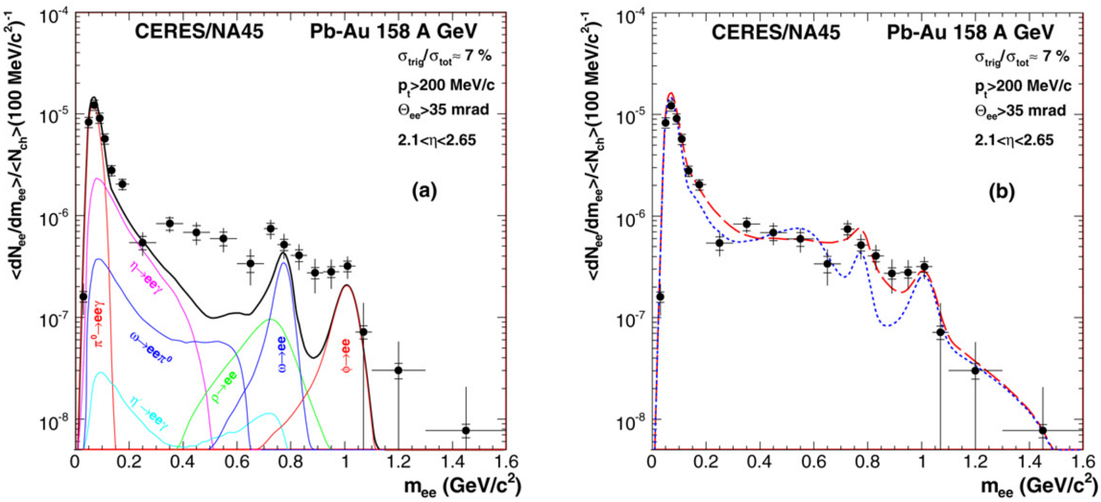


**Fig. 2.** (a) Invariant $e^+e^-$ mass spectrum compared to the expectation from hadronic decays. (b) The same data compared to calculations including a dropping $\rho$ mass (dashed) and a broadened $\rho$-spectral function (long-dashed). Systematic errors are indicated by horizontal ticks.

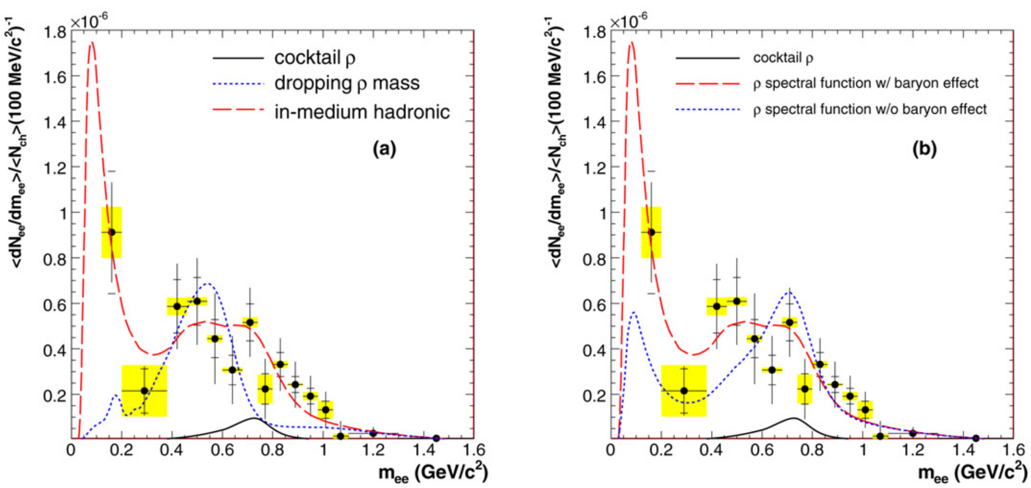


**Fig. 3.** $e^+e^-$ pair yield after subtraction of the hadronic cocktail. In addition to the statistical error bars, systematic errors of the data (horizontal ticks) and the systematic uncertainty of the subtracted cocktail (shaded boxes) are indicated. The broadening scenario (long-dashed line) is compared to a calculation assuming a density dependent dropping $\rho$ mass (dotted line in (a)) and to a broadening scenario excluding baryon effects (dotted line in (b)).

**Table 1**
Di-electron excess in $0.12 < m_{ee} < 1.1$ GeV/$c^2$ compared to model calculations

| | Data (± stat.) (± syst.) | In-medium hadronic | Dropping $\rho$ mass |
|---|---|---|---|
| Mean (GeV/$c^2$) | $0.54 \pm 0.07 \pm 0.01$ | 0.54 | 0.55 |
| Yield ($10^{-6}$) | $3.58 \pm 0.42 \pm 1.01$ | 3.88 | 2.41 |
| RMS (GeV/$c^2$) | $0.26 \pm 0.02 \pm 0.01$ | 0.25 | 0.18 |

in-medium hadronic spectral function approach and $P_{\mathrm{DRM}} = 10.1\%$ for the dropping $\rho$ mass scenario, the latter implying that the dropping $\rho$ mass scenario can be excluded on the $1.6\sigma$-level only. We note that, despite the statistical limitations of the present data, the discrimination power among the present model calculations is predominantly limited by systematic uncertainties.

A more detailed view may be derived by comparing the gross features of the data in Fig. 3(a) to the model calculations, see Table 1. The systematic errors on these quantities have been estimated by shifting each data point up or down by one standard deviation of its total systematic error. The mean values of the mass distributions of both calculations are in very good agreement with the measured excess data. The integrated yield in $0.12 < m_{ee} < 1.1$ GeV/$c^2$ agrees well with the in-medium hadronic spectral function approach, however, the systematic uncertainty does not exclude the dropping $\rho$ mass scenario either. In contrast, a comparison of the RMS widths clearly favors the in-medium hadronic spectral function approach, as the width of the data distribution is quite insensitive to systematic errors in scale of both data and cocktail. On this note, it is the large width observed in the data which drives the discrimination power among the model calculations.

The agreement of the data with the broadening scenario is strong evidence that the resonance structure of the $\rho$ meson is significantly modified in the hot and dense medium [16,25]. That $\rho$-related pair production is indeed a manifestation of the hot and dense matter created is supported by observing a particular mechanism at work which plays a dominant role in the hadronic spectral function approach: The strong coupling to baryons which adds strength to the di-electron yield at low masses [13]. The importance of this mechanism is demonstrated in Fig. 3(b), where the data are compared to in-medium hadronic spectral function calculations with and without baryon-induced interactions [16,24]. The calculations differ most in the mass range below 0.5 GeV/$c^2$, which is accessible with good efficiency by the present $e^+e^-$ data. The calculation omitting baryon effects falls short of the data for masses below 0.5 GeV/$c^2$ while inclusion of baryon interactions describes the measured low-mass yield very well. This is strong evidence that the observed modifications of the $\rho$-spectral function are foremost due to interactions with the dense baryonic medium.

It has been demonstrated that baryon-driven medium modifications lead to a low-mass di-electron spectrum which is very similar to the di-electron rate from lowest order perturbative $q\bar{q}$ annihilation [25]. Inspired by this apparent emergence of quark–hadron duality at low masses, Gallmeister et al. performed a calculation assuming that di-electron production via $q\bar{q}$ annihilation at $T_c$ is dominant [27]. That this phenomenological approach describes the shape of the measured distribution (Fig. 3) so well may be taken as an indication of chiral symmetry restoration which is implied in quark–hadron duality.

In cold nuclear matter, medium modifications not only of $\rho$ but also of $\omega$ and $\phi$ mesons have been observed [28–30] (see [31] for a recent review). Such modifications may also be present in the medium created in high-energy heavy-ion collisions. It should be noted however that the dominance of thermal two-pion annihilation to the total di-lepton yield via the $\rho$-channel disfavors a significant contribution from $\omega$ and $\phi$ to the observed di-lepton excess and its spectral distribution.

In conclusion, the present $e^+e^-$ data with improved mass resolution in the resonance region favor present models including a strong broadening of the $\rho$-spectral function in a hot and dense hadronic medium over a density dependent $\rho$ mass shift. Moreover, the $e^+e^-$ data at low pair mass and transverse momentum allow to test the relevance of baryonic effects to the modification of the $\rho$-spectral function. In comparison with models, the present CERES data suggest that baryonic interactions are important to explain the observed di-lepton yield at low masses.

## Acknowledgements

This work was supported by GSI, the German BMBF, the Virtual Institute VI-SIM of the German Helmholtz Association, the Israel Science Foundation, the Minerva Foundation and by the Grant Agency and Ministry of Education of the Czech Republic. We wish to thank Ralf Rapp for calculations and numerous discussions.

## References

[1] F. Karsch, Plenary talk at SciDAC 2006, J. Phys. Conf. Ser. 46 (2006) 122.
[2] P. Braun-Munzinger, Nucl. Phys. A 751 (2005) 127.
[3] M. Gyulassy, L. McLerran, Nucl. Phys. A 750 (2005) 30.
[4] I. Tserruya, Nucl. Phys. A 774 (2006) 415.
[5] J. Stachel, Int. J. Mod. Phys. A 21 (2006) 1750.
[6] R. Pisarski, Phys. Lett. B 110 (1982) 155.
[7] G.E. Brown, M. Rho, Phys. Rev. Lett. 66 (1991) 2720;
G.E. Brown, M. Rho, Phys. Rep. 269 (1996) 333.
[8] G. Agakichiev, et al., CERES Collaboration, Phys. Rev. Lett. 75 (1995) 1272.
[9] G. Agakichiev, et al., CERES Collaboration, Phys. Lett. B 422 (1998) 405.
[10] G. Agakichiev, et al., CERES Collaboration, Eur. Phys. J. C 41 (2005) 475.
[11] D. Adamova, et al., CERES Collaboration, Phys. Rev. Lett. 91 (2003) 042301.
[12] S. Afanasiev et al., PHENIX Collaboration, arXiv: 0706.3034, Phys. Rev. Lett., in press.
[13] R. Rapp, J. Wambach, Adv. Nucl. Phys. 25 (2000) 1.
[14] G.E. Brown, M. Rho, Phys. Rep. 363 (2002) 85.
[15] R. Arnaldi, et al., NA60 Collaboration, Phys. Rev. Lett. 96 (2006) 162302.
[16] H. van Hees, R. Rapp, Phys. Rev. Lett. 97 (2006) 102301.
[17] A. Marín, et al., CERES Collaboration, J. Phys. G: Nucl. Part. Phys. 30 (2004) S709;
D. Adamova, et al., CERES Collaboration, arXiv: 0802.1443 [nucl-ex], Nucl. Instrum. Methods, in press.
[18] S. Yurevich, doctoral thesis, University of Heidelberg, Germany, 2006.
[19] A. Cherlin, doctoral thesis, Weizmann Institute of Science, Rehovot, Israel, 2005.
[20] O. Busch, doctoral thesis, University of Darmstadt, Germany, 2007.
[21] D. Miśkowiec, et al., CERES Collaboration, Nucl. Phys. A 774 (2006) 43.
[22] D. Adamova, et al., CERES Collaboration, Phys. Rev. Lett. 96 (2006) 152301.
[23] W.-M. Yao, et al., Particle Data Group, J. Phys. G 33 (2006) 1.
[24] All calculations were performed by R. Rapp (private communication) based on [25].
[25] R. Rapp, J. Wambach, Eur. Phys. J. A 6 (1999) 415.
[26] G.E. Brown, J.W. Holt, C.H. Lee, M. Rho, Phys. Rep. 439 (2007) 161.
[27] K. Gallmeister, B. Kämpfer, O.P. Pavlenko, C. Gale, Nucl. Phys. A 688 (2001) 939,
B. Kämpfer, private communication.
[28] D. Trnka, et al., Phys. Rev. Lett. 94 (2005) 192203.
[29] M. Naruki, et al., KEK-E325 Collaboration, Phys. Rev. Lett. 96 (2006) 092301.
[30] R. Muto, et al., KEK-E325 Collaboration, nucl-ex/0511019.
[31] V. Metag, J. Phys. G: Nucl. Part. Phys. 34 (2007) S397.